

C.P. No. 407
(20,202)
A.R.C. Technical Report

LIBRARY
ROYAL AIRCRAFT ESTABLISHMENT
BEDFORD.

C.P. No. 407
(20,202)
A R.C. Technical Report



MINISTRY OF SUPPLY

AERONAUTICAL RESEARCH COUNCIL

CURRENT PAPERS

**THE THEORETICAL PERFORMANCES OF
SHOCK TUBES DESIGNED TO PRODUCE
HIGH SHOCK SPEEDS**

By

B. D. Henshall, B.Sc., Ph.D.
of the Aerodynamics Division, N.P.L.

LONDON : HER MAJESTY'S STATIONERY OFFICE

1958

PRICE 3s. 6d. NET

The Theoretical Performances of Shock Tubes
Designed to Produce High Shock Speeds

- By -

B. D. Henshall, B.Sc., Ph.D.
of the Aerodynamics Division, N.P.L.

30th May, 1958

SUMMARY

Ideal-gas calculations are made of the performance of a double diaphragm shock tube using hydrogen as the driver gas, argon in the intermediate section and air as the final driven gas. A comparison is made of the performance of the above shock tube with that of a single diaphragm shock tube using a hot hydrogen or combustion driver.

1. Introduction

For the simulation in a shock tube of re-entry into the Earth's atmosphere at very high speeds, it is necessary to generate shock Mach numbers* M_s up to 17. This upper limit on shock Mach number will simulate the velocity and stagnation temperature appropriate to the re-entry of an Earth Satellite. The production of strong shock waves is a difficult practical problem, and these extreme shock speeds have usually been attained^{1,2} by using "combustion" driver gases in the chamber of the shock tube. In this method a stoichiometric mixture of hydrogen and oxygen is ignited together with a helium diluent which forms about 75% of the total mass. [In some cases hydrogen has been used as the diluent.]

Particularly for large shock tubes, it is difficult to achieve controlled and complete burning without detonation: many experimental programmes³ have been carried out to determine optimum mixing and igniting procedures and mixture compositions. Such studies have shown that combustion drivers are naturally erratic, and that a practical solution for one shock tube will not necessarily hold for another. It was with these facts in mind that the present study was initiated.

The theory of multiple diaphragm shock tubes using air throughout as the working fluid has been previously described⁴ by the present writer, and in this paper the results of Ref. 4 are simply modified to extend the calculations to the special case of a double-diaphragm shock tube with cold hydrogen driving argon which in turn finally drives air. This configuration can be conveniently denoted by $(H_2 \rightarrow A \rightarrow \text{Air})$. It is shown that the performance of such a shock tube is comparable to that of a single diaphragm shock tube using a combustion driver and having the same overall diaphragm pressure ratio.

Equations which were given and used in Ref. 4 are quoted below without derivation: details of the notation used are given in the Appendix to this report.

2./

*For notation, see Appendix.

2. The Single-Diaphragm Shock Tube

The general shock tube performance equation is

$$P_o = \left\{ \frac{2\gamma_1}{\gamma_1 + 1} M_{S_1}^2 - \frac{\gamma_1 - 1}{\gamma_1 + 1} \right\} \left\{ 1 - \frac{a_1}{a_4} \left(\frac{\gamma_1 - 1}{\gamma_1 + 1} \right) \left(\frac{M_{S_1}^2 - 1}{M_{S_1}} \right) \right\}^{-\frac{2\gamma_4}{\gamma_4 - 1}} \dots(1)$$

where suffix ₁ refers to conditions in the channel (driven gas)

suffix ₄ refers to conditions in the chamber (driver gas)

$$P_o = \frac{P_4}{P_1} = P_{4,1} \quad \text{the overall diaphragm pressure ratio}$$

$$T_o = \frac{T_4}{T_1} = T_{4,1} \quad \text{the overall diaphragm temperature ratio}$$

$$\text{and} \quad \frac{a_1}{a_4} = T_o^{-\frac{1}{2}} \sqrt{\frac{\gamma_1 m_4}{\gamma_4 m_1}} \dots(2)$$

A flow diagram for a single diaphragm shock tube which illustrates the nomenclature used in this report is given in Fig. 1. Various combinations of driver and driven gases are given in the following sections.

2.1 H₂ → Air shock tube with T_o = 1

In this case $\gamma_4 = \gamma_1 = 1.40$, $m_4 = 2$, $m_1 = 29$ and equation (1) reduces to

$$P_o = \left\{ \frac{7M_{S_1}^2 - 1}{6} \right\} \left\{ 1 - \frac{1}{6} \sqrt{\frac{2}{29}} \left(\frac{M_{S_1}^2 - 1}{M_{S_1}} \right) \right\}^{-7} \dots(3)$$

Table I gives the values of P_o calculated from equation (2) for a range of M_{S_1} values from 1 to 17.7 in steps of 0.1. A shock Mach number of 17 requires an initial pressure ratio across the diaphragm of 4.4×10^6 . A curve of P_o versus M_{S_1} is given in Fig. 2.

2.2 H₂ → Air shock tube with T_o variable

Equation (1) becomes

$$P_o = \left\{ \frac{7M_{S_1}^2 - 1}{6} \right\} \left\{ 1 - \frac{T_o^{-\frac{1}{2}}}{6} \sqrt{\frac{2}{29}} \left(\frac{M_{S_1}^2 - 1}{M_{S_1}} \right) \right\}^{-7} \dots(4)$$

It is possible to envisage the use of a hot hydrogen driver for a shock tube; a value of $T_o = 4$ is a probable upper limit for this mode of operation. Calculations of P_o have been made from equation (4) for the cases $T_o = 2, 3$ and 4 for a range of shock Mach numbers from 1 to 25 in unit steps. These values are given in Table II and plotted, together with the $T_o = 1$ curve, as Fig. 2. It is immediately obvious that for the same overall pressure ratio a much faster shock wave is produced by hot hydrogen driver gas than cold hydrogen driver gas.

2.3 Combustion → Air shock tube

The AVCO Research Laboratory have illustrated¹ the performance of a combustion driven shock tube. They found that $\gamma_4 = 1.60$ and $a_4/a_1 = 7.3$ effectively and thus equation (1) becomes, for $\gamma_1 = 1.40$,

$$P_o = \left\{ \frac{7M_{S_1}^2 - 1}{6} \right\} \left\{ 1 - \frac{1}{29.2} \left(\frac{M_{S_1}^2 - 1}{M_{S_1}} \right) \right\}^{-5.33} \dots (5)$$

Table III shows the results of calculations of P_o made from equation (5) for a range of values of M_{S_1} from 1 to 25 in unit steps. The 'performance-curve' of P_o versus M_{S_1} for a combustion-driven shock tube is compared with those for hydrogen-driven shock tubes in Fig. 2.

3. Preliminary Calculations for a $H_2 \rightarrow$ Argon \rightarrow Air Shock Tube

Some preliminary calculations which must be made before the performance of a $H_2 \rightarrow$ Argon \rightarrow Air shock tube can be evaluated are given in this section. We require the individual details of the performance of $H_2 \rightarrow$ Argon ($T_o = 1$) and Argon \rightarrow Air (variable T_o) shock tubes before we can combine them with the results for the reflection of a shock wave from a rigid wall to predict the complete performance of the $H_2 \rightarrow$ Argon \rightarrow Air double diaphragm reflected type shock tube. The wave diagram for such a shock tube is given in Fig. 3; the various flow regions are identified by numerical suffices to all quantities.

The primary shock wave M_{S_3} , which is produced by the rupture of diaphragm D_1 between the hydrogen and the argon, undergoes normal reflection at diaphragm D_2 and leaves the argon in region 4 at rest at an increased temperature and pressure (with respect to its initial state in region 6). After a predetermined delay, diaphragm D_2 is ruptured, and the ensuing flow produces a shock wave M_{S_4} appropriate to the single diaphragm Argon \rightarrow Air shock tube where the effective pressure and temperature ratios across the diaphragm are p_{41} and T_{41} .

The relations between p_{81} and p_{41} , T_{61} ($= T_{68} = T_o = 1$) and T_{41} are obtained from the results of the reflection of a shock wave from a rigid wall. These individual calculations will now be made, and their combined use is illustrated in Section 4 below.

3.1 $H_2 \rightarrow$ Argon shock tube with $T_{68} = 1$

The notation of Fig. 3 is adopted and then equation (1) applies with $\gamma_8 = 1.40$ $\gamma_6 = 1.67$ $m_8 = 2$ and $m_6 = 40$. Then

$$p_{88} = \left\{ \frac{5M_{S_6}^2 - 1}{4} \right\} \left\{ 1 - \frac{3}{20} \sqrt{\frac{2}{40}} \sqrt{\frac{25}{21}} \left(\frac{M_{S_6}^2 - 1}{M_{S_6}} \right) \right\}^{-7} \dots (6)$$

Calculations of p_{88} values from equation (6) for a range of M_{S_6} values from 1 to 20 in unit steps are presented in Table IV and are plotted in Fig. 4. The particular variations of p_{88} with M_{S_6} for the cases $H_2 \rightarrow$ Helium and $H_2 \rightarrow$ Xenon are also shown in Fig. 4 for comparison with the $H_2 \rightarrow$ Argon curve. (In all cases $T_{68} = 1$.)

3.2 The reflection of a normal shock wave from a rigid wall

From shock wave theory, the relations between the pressure and temperature in the effective reservoir (region 4 of Fig. 3) and the original conditions in the argon chamber (region 6) are given by

$$p_{46} = \left\{ \frac{2\gamma_6}{\gamma_6 + 1} M_{S_6}^2 - \frac{\gamma_6 - 1}{\gamma_6 + 1} \right\} \left\{ \frac{(3\gamma_6 - 1) M_{S_6}^2 - 2(\gamma_6 - 1)}{(\gamma_6 - 1) M_{S_6}^2 + 2} \right\} \dots (7)$$

$$\text{and } T_{46} = \frac{\{(3\gamma_6 - 1) M_{S_6}^2 - 2(\gamma_6 - 1)\} \{2(\gamma_6 - 1) M_{S_6}^2 + (3 - \gamma_6)\}}{(\gamma_6 + 1)^2 M_{S_6}^2} \dots (8)$$

When/

When $\gamma_6 = 1.67$ as in this case for argon, equations (7) and (8) become

$$P_{46} = \left[\frac{5M_{S_6}^2 - 1}{2} \right] \left[\frac{3M_{S_6}^2 - 1}{M_{S_6}^2 + 3} \right] \quad \dots(9)$$

and

$$T_{46} = \frac{(3M_{S_6}^2 - 1)(M_{S_6}^2 + 1)}{4M_{S_6}^2} \quad \dots(10)$$

From equations (9) and (10) calculations of P_{46} and T_{46} were made for a range of M_{S_6} values from 1 to 30 in unit steps and the results are reproduced as Table V.

3.3 Argon → Air shock tube with T_{41} variable

The final shock wave M_{S_1} produced by the $H_2 \rightarrow$ Argon \rightarrow Air double diaphragm shock tube shown in Fig. 3 is actually that of a single diaphragm Argon \rightarrow Air shock tube with an initial pressure ratio P_{41} , and an initial temperature ratio T_{41} , across the diaphragm D_2 . Therefore, equation (1) can be applied with $\gamma_4 = 1.67$, $\gamma_1 = 1.40$, $m_4 = 40$ and $m_1 = 29$. Then

$$P_{41} = \left\{ \frac{7M_{S_1}^2 - 1}{6} \right\} \left\{ 1 - \frac{5}{18} T_{41}^{-\frac{1}{2}} \sqrt{\frac{40}{29}} \sqrt{\frac{21}{25}} \left(\frac{M_{S_1}^2 - 1}{M_{S_1}} \right) \right\}^{-5} \quad \dots(11)$$

Values of p_{41} were calculated from equation (11) for independent ranges of M_{S_1} values from 5 to 20 in unit steps and of T_{41} values from 10 to 200 in steps of 10. Table VI gives the results of these calculations and Fig. 5 illustrates the overall variation of M_{S_1} with T_{41} and P_{41} for the Argon \rightarrow Air shock tube.

4. The Performance of a $H_2 \rightarrow$ Argon \rightarrow Air Double Diaphragm Shock Tube

An example of the method used to calculate the performance of a $H_2 \rightarrow$ Argon \rightarrow Air shock tube is given below. Let us refer to Fig. 3, and suppose that the overall pressure ratio across the extreme ends of the shock tube $P_0 = p_{81} = 3 \times 10^4$, and that the initial temperature is constant throughout the tube, that is, $T_0 = 1$. From Table I we note that the shock Mach number M_{S_1} corresponding to $P_0 = 3 \times 10^4$, $T_0 = 1$ for a single diaphragm $H_2 \rightarrow$ Air shock tube is 12.0. Now consider the effect of the insertion of the second diaphragm D_2 , and the variation of the intermediate pressure p_6 of argon. For example, let $p_{81} = 10$. The p_{86} is known since

$$P_0 = p_{86} \cdot p_{81} = 3 \times 10^4.$$

Firstly, the shock Mach number M_{S_6} is found from the $H_2 \rightarrow$ Argon results of Table IV and Fig. 4. If $p_{86} = 3 \times 10^3$, $M_{S_6} = 10.05$. The p_4 and T_4 are found from the general reflected shock Table V; the numerical values are

$$P_{46} = 732 \text{ and } T_{46} = 76.5.$$

Thus $p_{41} = p_{46} \cdot p_{61} = 7320$ is determined, and the final shock Mach number M_{S_1} ($= 14.4$) is obtained by an interpolation from Table VI or Fig. 5. This procedure may be repeated for any value of p_6 ; similar calculations may be made for other values of P_0 .

Fig. 6 reproduces the results of calculations made for values of $P_0 = 5 \times 10^2, 10^3, 5 \times 10^3, 10^4, 3 \times 10^4, \text{ and } 10^5$. It is clear

that/

that a considerable increase in the attainable shock Mach number is possible by a suitable choice of the intermediate pressure ratio P_{s1} . Since the actual p_{s1} values are quite small, the second diaphragm would be a light plastic membrane in practice.

5. Discussion of Results

Fig. 6 illustrates that for any value of the overall pressure ratio P_0 there exists an optimum value of the argon/air pressure ratio P_{s1} for which the final shock Mach number M_{s1} is a maximum. Figs. 7 and 8 are cross plots from Fig. 6 and show that the variation of $(P_{s1})_{\text{optimum}}$ with $(M_{s1})_{\text{max}}$ and P_0 respectively is linear.

The performances of $H_2 \rightarrow \text{Air}$ ($T_0 = 1$), Combustion \rightarrow Air and optimum $H_2 \rightarrow \text{Argon} \rightarrow \text{Air}$ shock tubes are compared in Fig. 9.

An engineering limit on P_0 is usually 10^6 for structural considerations, and at $P_0 = 10^5$ the three types of shock tubes give values of M_{s1} of 13.4, 18.8 and 17.3 respectively. Thus we note that the optimum $H_2 \rightarrow \text{Argon} \rightarrow \text{Air}$ shock tube can produce the highest shock Mach number (= 17) required to simulate the velocity and stagnation enthalpy appropriate to the re-entry of an Earth Satellite into the atmosphere. Furthermore, all the experimental difficulties encountered in the combustion process are circumvented.

If some method of uniformly heating hydrogen in the chamber of a single diaphragm shock tube can be devised, it would seem that this mode of shock tube operation is the most attractive of all. If the chamber temperature is only 600°K ($T_0 \approx 2$), then an overall pressure ratio P_0 of 10^5 will produce a shock Mach number of 17.8. Until constant chamber conditions can be produced by heating hydrogen, the double diaphragm $H_2 \rightarrow \text{Argon} \rightarrow \text{Air}$ shock tube would appear to be an attractive method of shock tube technique, particularly at high overall pressure ratios. Finally, it may be noted that no burning at a hydrogen-air contact surface can occur in the $H_2 \rightarrow \text{Argon} \rightarrow \text{Air}$ shock tube.

Since the intermediate chamber length will be approximately 2 to 3 times the main chamber length, the running time of a $H_2 \rightarrow \text{Argon} \rightarrow \text{Air}$ shock tube will be about 30% shorter than that of a single diaphragm shock tube of the same overall length.

6. Conclusion

It has been shown that an optimum double diaphragm $H_2 \rightarrow \text{Argon} \rightarrow \text{Air}$ shock tube can simulate the velocity and stagnation enthalpy appropriate to the re-entry of an Earth Satellite into the atmosphere. This type of shock tube does not have the experimental difficulties encountered with a combustion-driver shock tube and associated with controlled and complete burning of combustible gas mixtures in the chamber of the shock tube.

Acknowledgements

Mrs. N. A. North and Mrs. C. M. Stuart performed the computations.

References/

References

<u>No.</u>	<u>Author(s)</u>	<u>Title, etc.</u>
1	P. H. Rose	Physical gasdynamic research at AVCO Research Laboratory. AVCO Research Laboratory Research Note 37. May, 1957.
2	C. E. Wittliff and M. R. Wilson	Shock tube driver techniques and attenuation measurements. Cornell Aero. Lab. Rept. AD-1052-A-4. August, 1957.
3	G. F. Anderson	Shock tube operation with combustible driver gases. AVCO Research Laboratory. (Private communication March, 1957).
4	B. D. Henshall	The use of multiple diaphragms in shock tubes. C.P.291. 3rd December, 1955.

APPENDIX/

APPENDIX

Notation

a	velocity of sound
m	molecular weight
P	absolute pressure
R	the gas constant
t	time
T	absolute temperature
u	flow velocity
U	shock velocity; subscript corresponds to flow region <u>ahead</u> of shock
x	distance measured along longitudinal axis of shock tube
y	the ratio of the specific heats
$M_{s()}$	shock wave propagation Mach number with respect to the speed of sound in the flow <u>ahead</u> of the shock front (e.g., $M_{s_1} = U_1/a_1$)
P_0	overall pressure ratio across extreme ends of any type of shock tube
T_0	overall temperature ratio across extreme ends of any type of shock tube.

Subscripts

1, 2, 3, 4, 5, etc. identify quantities related to gas in corresponding region of shock tube flow (see Figures).

Special Non-dimensional Notation

$$P_{mn} = \frac{P_m}{P_n} \quad \text{a pressure ratio}$$
$$T_{mn} = \frac{T_m}{T_n} \quad \text{a temperature ratio.}$$

TABLE I/

TABLE I

Hydrogen → Air Shock Tube with $T_0 = 1$

M_{S_1}	P_0	M_S	P_0	M_S	P_0
1.0	1.0	6.6	515.83	12.2	34,451
1.1	1.3211	6.7	555.78	12.3	37,394
1.2	1.6935	6.8	598.27	12.4	40,625
1.3	2.1271	6.9	644.17	12.5	44,146
1.4	2.6242	7.0	692.80	12.6	48,018
1.5	3.1886	7.1	745.94	12.7	52,227
1.6	3.8274	7.2	802.61	12.8	56,859
1.7	4.5456	7.3	862.98	12.9	61,932
1.8	5.3493	7.4	928.53	13.0	67,484
1.9	6.2416	7.5	998.16	13.1	73,621
2.0	7.2409	7.6	1073.8	13.2	80,298
2.1	8.3426	7.7	1154.0	13.3	87,681
2.2	9.5588	7.8	1241.7	13.4	95,786
2.3	10.897	7.9	1334.4	13.5	104,730
2.4	12.379	8.0	1435.8	13.6	114,550
2.5	13.990	8.1	1543.5	13.7	125,400
2.6	15.769	8.2	1660.4	13.8	137,400
2.7	17.746	8.3	1784.1	13.9	150,690
2.8	19.815	8.4	1917.8	14.0	165,350
2.9	22.116	8.5	2063.9	14.1	181,550
3.0	24.621	8.6	2218.2	14.2	199,580
3.1	27.384	8.7	2387.2	14.3	219,430
3.2	30.339	8.8	2566.3	14.4	241,660
3.3	33.559	8.9	2760.0	14.5	266,070
3.4	37.034	9.0	2967.6	14.6	293,490
3.5	40.851	9.1	3195.3	14.7	323,970
3.6	44.906	9.2	3436.4	14.8	358,010
3.7	49.363	9.3	3694.9	14.9	396,090
3.8	54.138	9.4	3887.7	15.0	438,230
3.9	59.362	9.5	4283.6	15.1	485,850
4.0	64.878	9.6	4613.2	15.2	538,900
4.1	70.958	9.7	4963.6	15.3	598,550
4.2	77.393	9.8	5351.7	15.4	665,420
4.3	84.430	9.9	5762.4	15.5	740,960
4.4	91.960	10.0	6205.9	15.6	826,040
4.5	100.12	10.1	6689.6	15.7	921,510
4.6	108.87	10.2	7204.4	15.8	1,029,900
4.7	118.33	10.3	7777.0	15.9	1,152,100
4.8	128.47	10.4	8383.1	16.0	1,290,900
4.9	139.35	10.5	9044.8	16.1	1,445,100
5.0	151.11	10.6	9749.9	16.2	1,623,300
5.1	163.72	10.7	10525.0	16.3	1,826,400
5.2	177.37	10.8	11358	16.4	2,058,300
5.3	191.91	10.9	12282	16.5	2,324,300
5.4	207.54	11.0	13261	16.6	2,626,600
5.5	224.55	11.1	14332	16.7	2,975,800
5.6	242.60	11.2	15488	16.8	3,375,200
5.7	262.00	11.3	16742	16.9	3,838,000
5.8	282.82	11.4	18113	17.0	4,368,200
5.9	305.28	11.5	19588	17.1	4,986,500
6.0	329.30	11.6	21199	17.2	5,697,700
6.1	355.22	11.7	22957	17.3	6,529,800
6.2	383.00	11.8	24906	17.4	7,478,300
6.3	412.86	11.9	27002	17.5	8,604,000
6.4	444.93	12.0	29262	17.6	9,924,300
6.5	479.41	12.1	31755	17.7	11,473,000

TABLE II

H₂ → Air Shock Tube Using Hot Hydrogen as the Driver Gas

M _{a1}	Overall diaphragm pressure ratio P ₀			
	T ₀ = 1	T ₀ = 2	T ₀ = 3	T ₀ = 4
1	1.0	1.0	1.0	1.0
2	7.241	6.276	5.897	5.683
3	26.62	18.87	16.84	15.74
4	64.88	43.89	37.14	33.70
5	151.1	89.35	71.70	63.05
6	329.3	168.5	127.7	108.8
7	692.8	302.7	216.0	178.0
8	1436	526.4	352.2	279.9
9	2968	896.8	559.8	428.8
10	6206	1509	874.4	643.4
11	13,260	2520	1348	951.5
12	29,260	4203	2060	1392
13	67,480	7029	3134	2018
14	165,300	11,850	4762	2912
15	438,200	20,160	7226	4185
16	1,291,000	34,760	11,010	6012
17	4,368,000	61,140	16,840	8622
18	-	110,000	25,920	12,400
19	-	203,300	40,290	17,870
20	-	388,800	63,260	25,890
21	-	774,300	100,600	37,670
22	-	1,625,000	162,900	55,270
23	-	3,620,000	268,000	81,680
24	-	-	450,900	121,900
25	-	-	743,000	183,900

TABLE III

Combustion → Air Shock Tube

$\gamma_4 = 1.60, \gamma_1 = 1.40. a_4/a_1 = 7.3$ in Equation (1)

Shock Mach Number M_{S_1}	Overall Diaphragm Pressure Ratio P_0
1	1.0
2	5.962
3	17.21
4	38.50
5	75.58
6	137.3
7	237.6
8	398.3
9	653.9
10	1060
11	1709
12	2751
13	4448
14	7248
15	11,960
16	20,090
17	34,510
18	60,970
19	111,900
20	214,400
21	435,700
22	955,700
23	2,310,000
24	6,390,000
25	21,490,000

TABLE IV/

TABLE IV

Hydrogen → Argon Shock Tube

Shock Mach Number M_{S_1}	Overall Diaphragm Pressure Ratio P_0
1	1.0
2	7.052
3	22.57
4	55.49
5	119.8
6	240.2
7	460.8
8	858.6
9	1585
10	2905
11	5309
12	9899
13	18,620
14	35,880
15	71,120
16	146,300
17	315,000
18	718,800
19	1,766,000
20	4,778,000

TABLE V/

TABLE V

The Reflection of a Shock Wave from a Rigid Wall

$$\gamma = 1.67$$

Shock Mach Number M_{S_6}	P_{4_6} Eqn. (9)	T_{4_6} Eqn. (10)
1	1.0	1.0
2	14.93	3.44
3	47.67	7.72
4	97.71	12.48
5	163.9	19.24
6	245.6	27.49
7	342.5	37.24
8	454.7	48.50
9	582.0	61.25
10	724.3	75.50
11	881.6	91.25
12	1,054	108.5
13	1,241	127.2
14	1,444	147.5
15	1,661	169.2
16	1,894	192.5
17	2,141	217.2
18	2,404	243.5
19	2,681	271.2
20	2,974	300.5
21	3,281	331.2
22	3,604	363.5
23	3,941	397.3
24	4,294	432.5
25	4,661	469.3
26	5,044	507.5
27	5,441	547.3
28	5,854	588.5
29	6,281	631.3
30	6,724	675.5

TABLE VI/

TABLE VI

[Equation (11)].- Argon → Air Shock Tube

Values of p_{41} for independent ranges of M_{S_6} and T_{41}

T_{41} \ M_{S_6}	10	20	30	40	50	60	70	80	90	100
5	597.2	201.0	132.6	105.1	90.18	80.82	74.34	69.55	65.86	62.92
6	2310	495.6	284.5	210.0	172.5	149.8	134.7	123.7	115.6	109.0
7	10,620	1225	594.8	404.4	315.9	265.3	232.5	209.7	192.7	179.6
8	68,690	3134	1238	765.3	564.8	456.1	389.1	343.3	310.4	285.3
9	906,150	8592	2615	1441	996.3	771.8	638.0	550.2	488.2	442.2
10	-	26,410	5694	2737	1755	1294	1035	869.4	756.3	674.1
11	-	97,390	13,050	5298	3111	2171	1668	1363	1160	1015
12	-	485,600	32,270	10,590	5590	3658	2691	2130	1770	1520
13	-	-	89,080	22,140	10,280	6235	4367	3335	2696	2267
14	-	-	289,900	49,280	19,510	10,830	7161	5248	4116	3378
15	-	-	-	119,600	38,650	19,280	11,910	8335	6318	5054
16	-	-	-	328,600	81,190	35,430	20,240	13,430	9784	7600
17	-	-	-	-	184,000	68,060	35,270	21,990	15,340	11,520
18	-	-	-	-	463,800	138,100	63,710	36,900	24,450	17,680
19	-	-	-	-	-	301,600	120,100	63,670	39,750	27,530
20	-	-	-	-	-	727,800	240,000	113,900	66,280	43,660

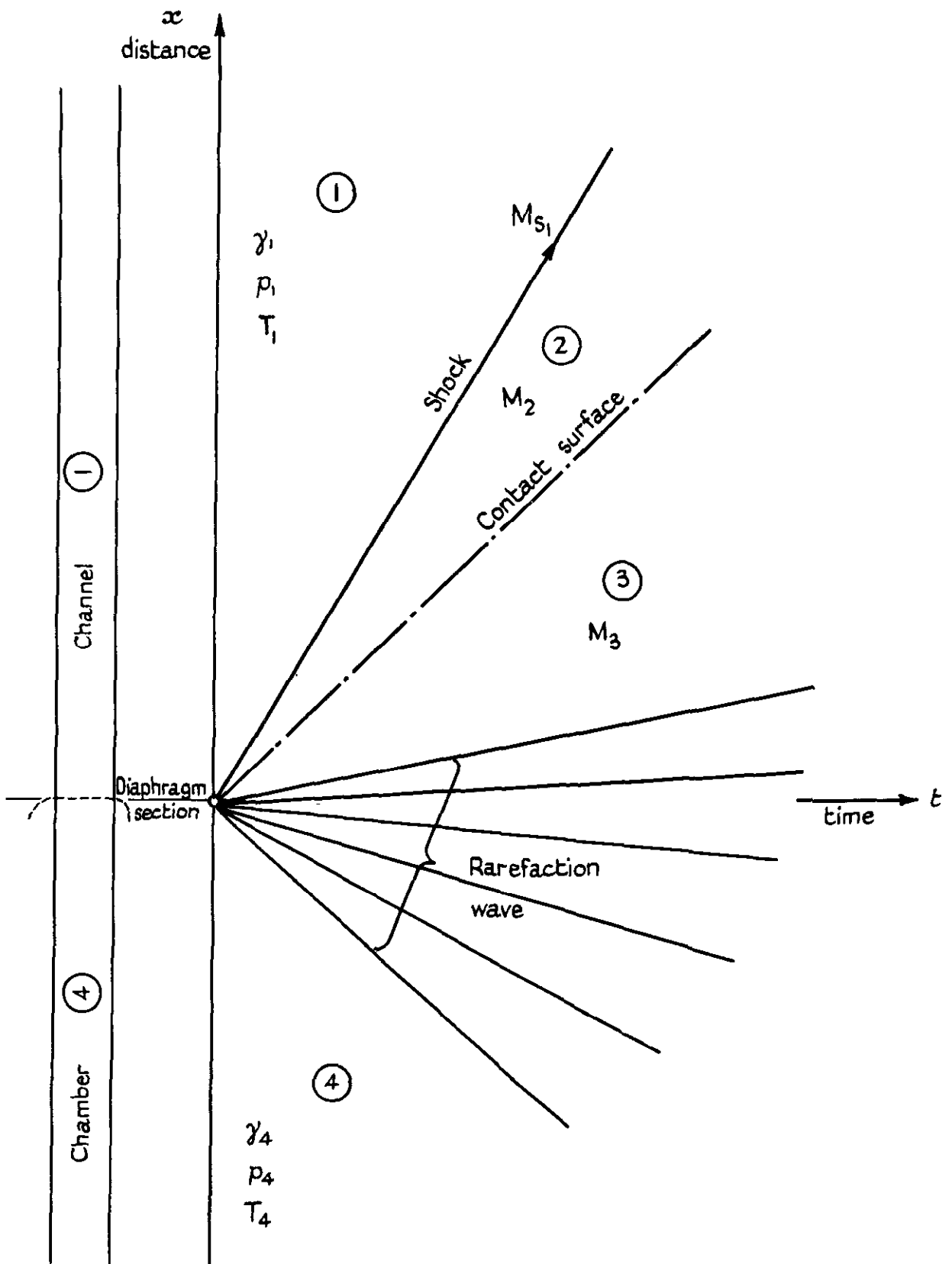
- 13 -

TABLE VI (Contd.)

TABLE VI (Contd.)

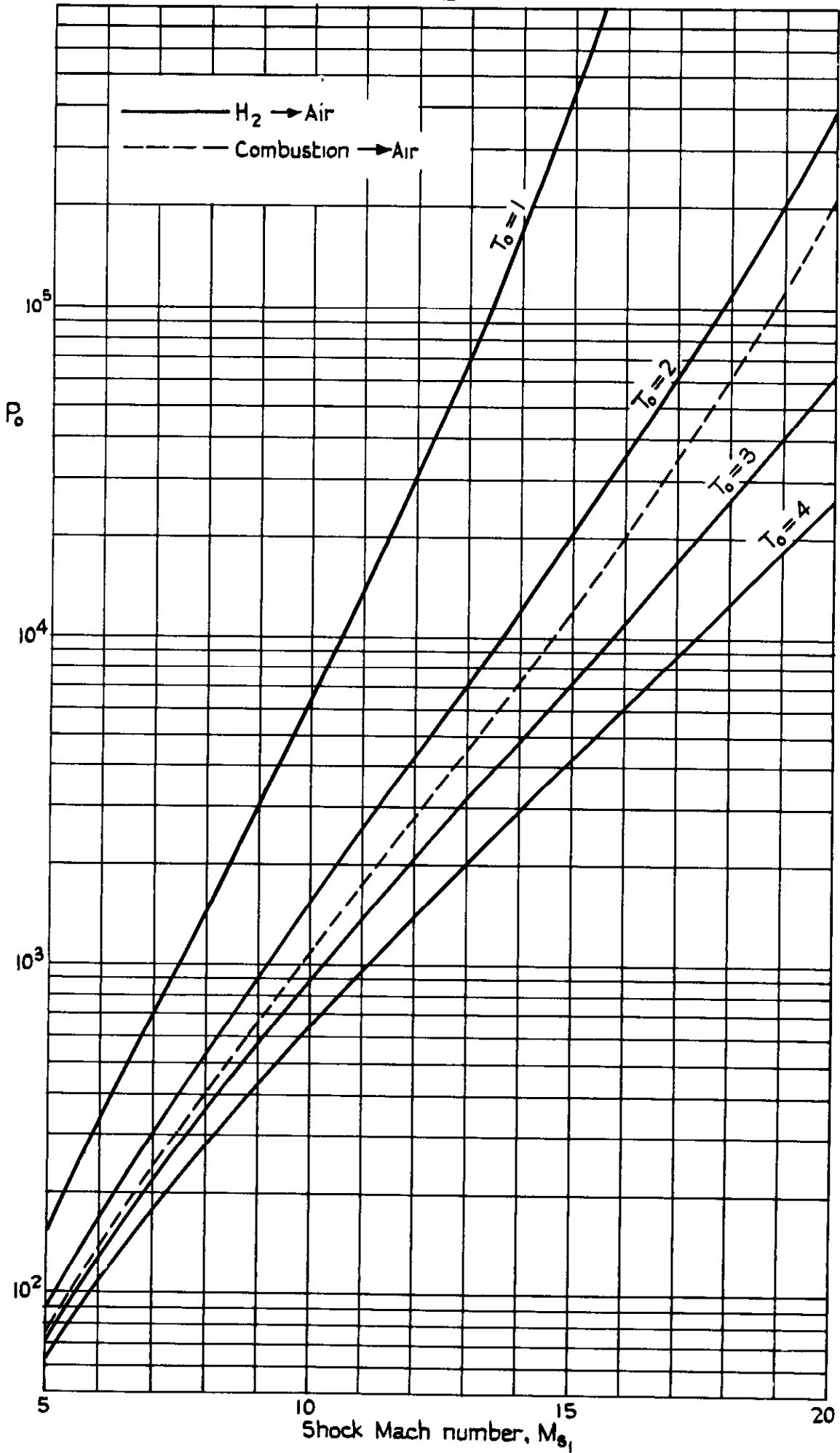
T_{41} M_{S_1}	110	120	130	140	150	160	170	180	190	200
5	60.55	58.52	56.83	55.36	54.09	52.97	51.96	51.07	50.25	49.52
6	103.9	99.61	95.96	92.83	90.16	87.82	85.78	83.93	82.30	80.82
7	169.1	160.7	153.6	147.6	142.5	138.0	134.1	130.7	127.6	124.5
8	265.8	249.9	236.8	226.1	216.7	208.7	201.7	195.5	190.2	185.2
9	406.9	378.7	355.6	336.7	320.7	307.0	295.0	284.5	275.5	267.2
10	611.8	563.1	524.0	491.5	464.6	442.1	422.4	405.3	390.3	377.1
11	908.7	825.8	760.3	707.3	663.7	626.5	595.0	567.9	544.3	523.2
12	1338	1200	1092	1007	936.7	878.2	827.9	785.4	749.2	716.6
13	1962	1735	1560	1424	1312	1220	1142	1078	1021	972.1
14	2871	2500	2219	2002	1826	1684	1566	1466	1381	1307
15	4203	3598	3149	2806	2533	2315	2135	1985	1858	1749
16	6180	5189	4471	3930	3512	3176	2905	2680	2491	2330
17	9133	7511	6359	5513	4864	4351	3945	3608	3332	3095
18	13,610	10,940	9084	7757	6752	5975	5357	4859	4447	4108
19	20,510	16,070	13,060	10,960	9402	8215	7286	6548	5943	5445
20	31,330	23,850	18,930	15,590	13,140	11,340	9938	8837	7947	7224

Fig. 1



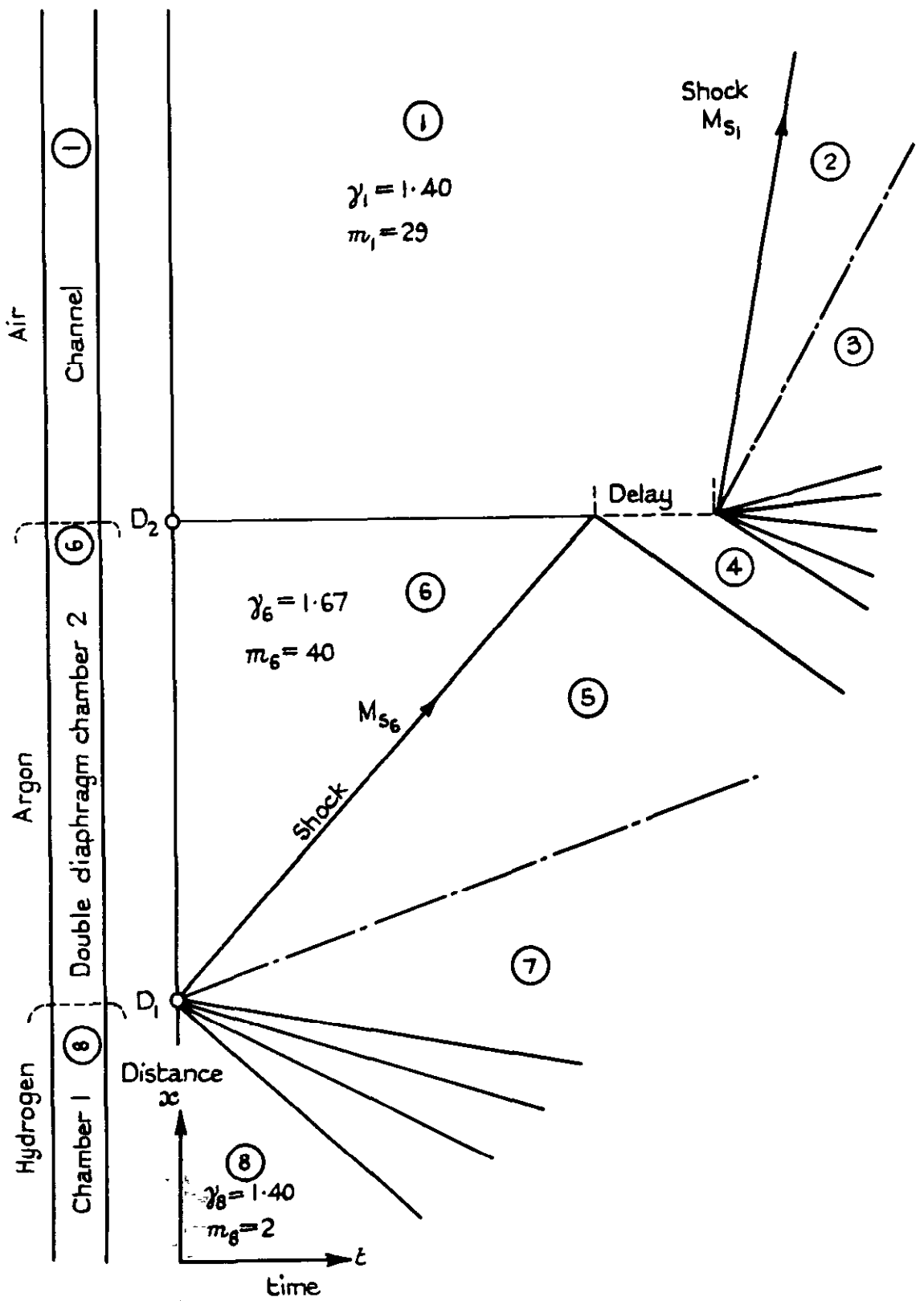
A simple shock tube: Flow diagram

FIG 2.



Comparison of combustion and hydrogen driver shock tubes. (Driven gas in air)

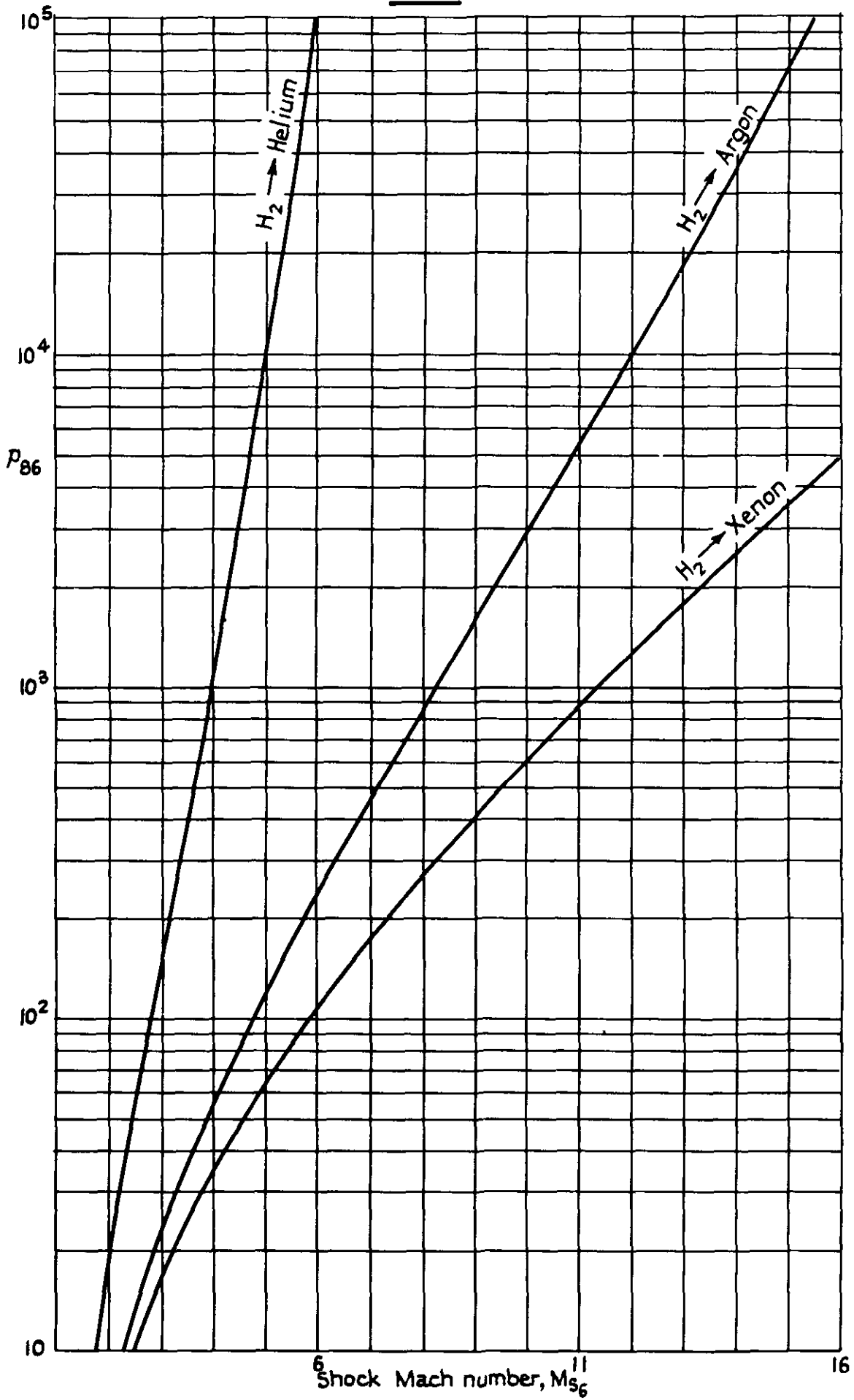
FIG. 3.



Double - diaphragm shock tube - reflected shock type: flow diagram

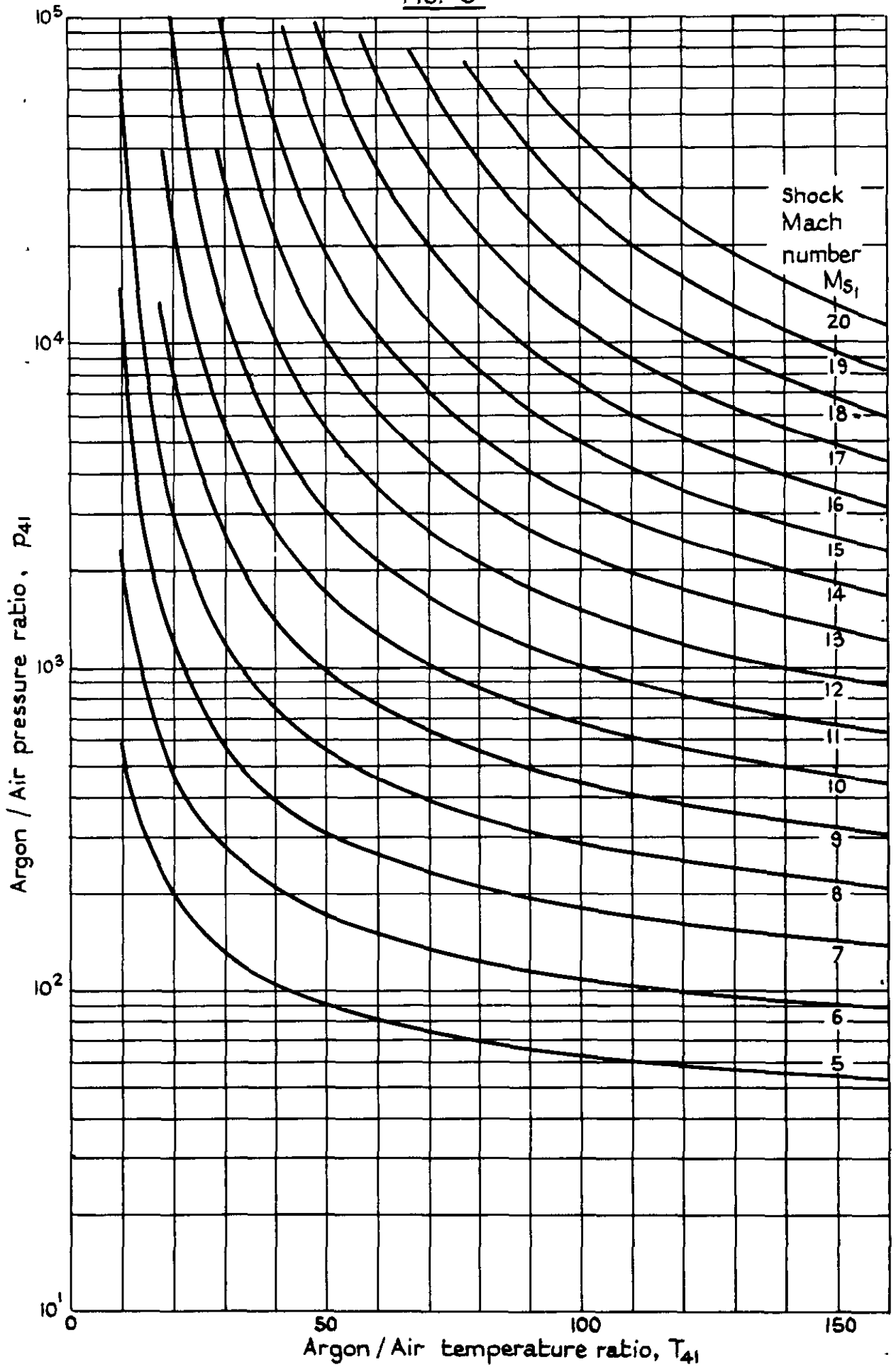
H₂ → Argon → Air

FIG. 4.



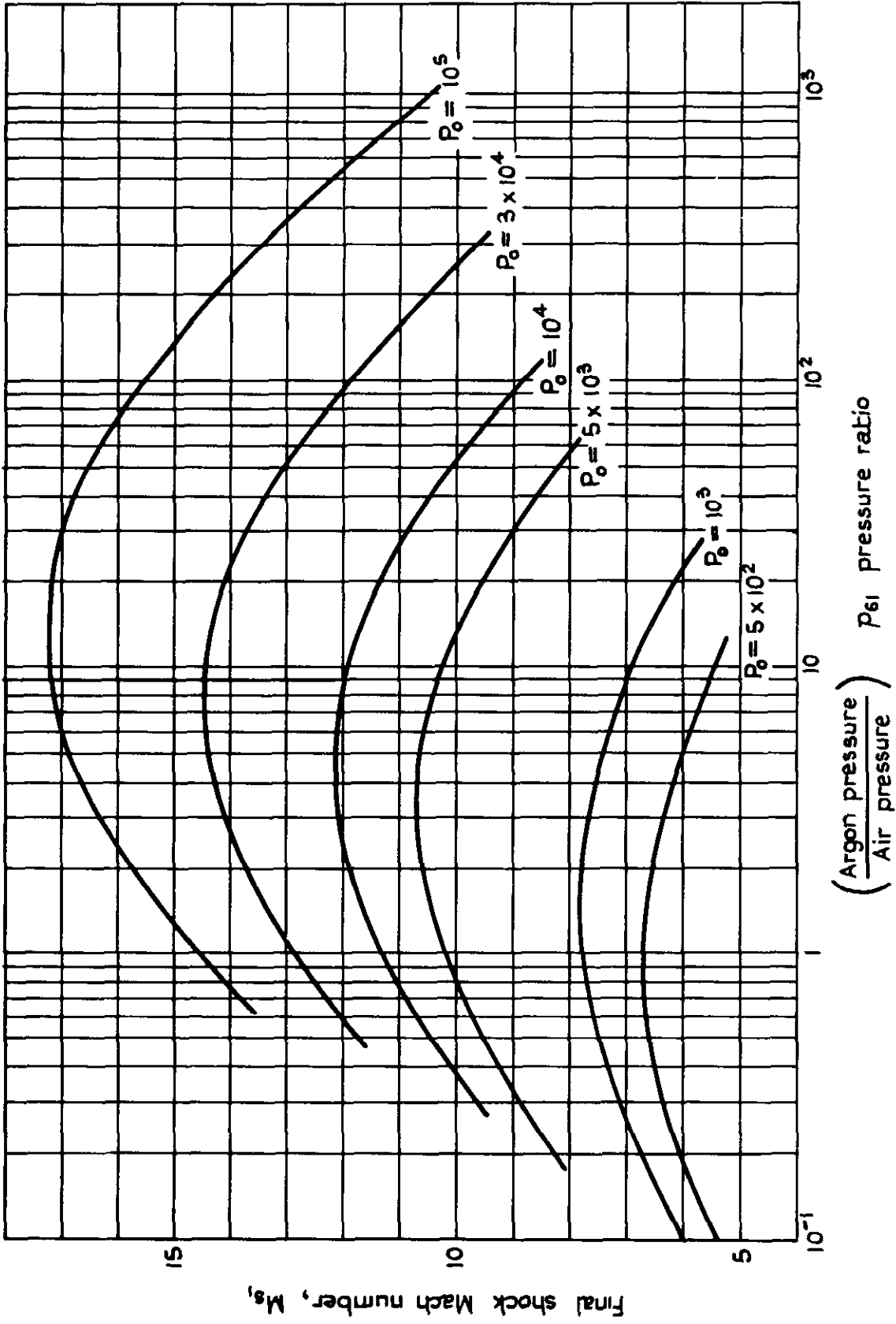
Hydrogen driving inert gases in shock tubes

Fig. 5



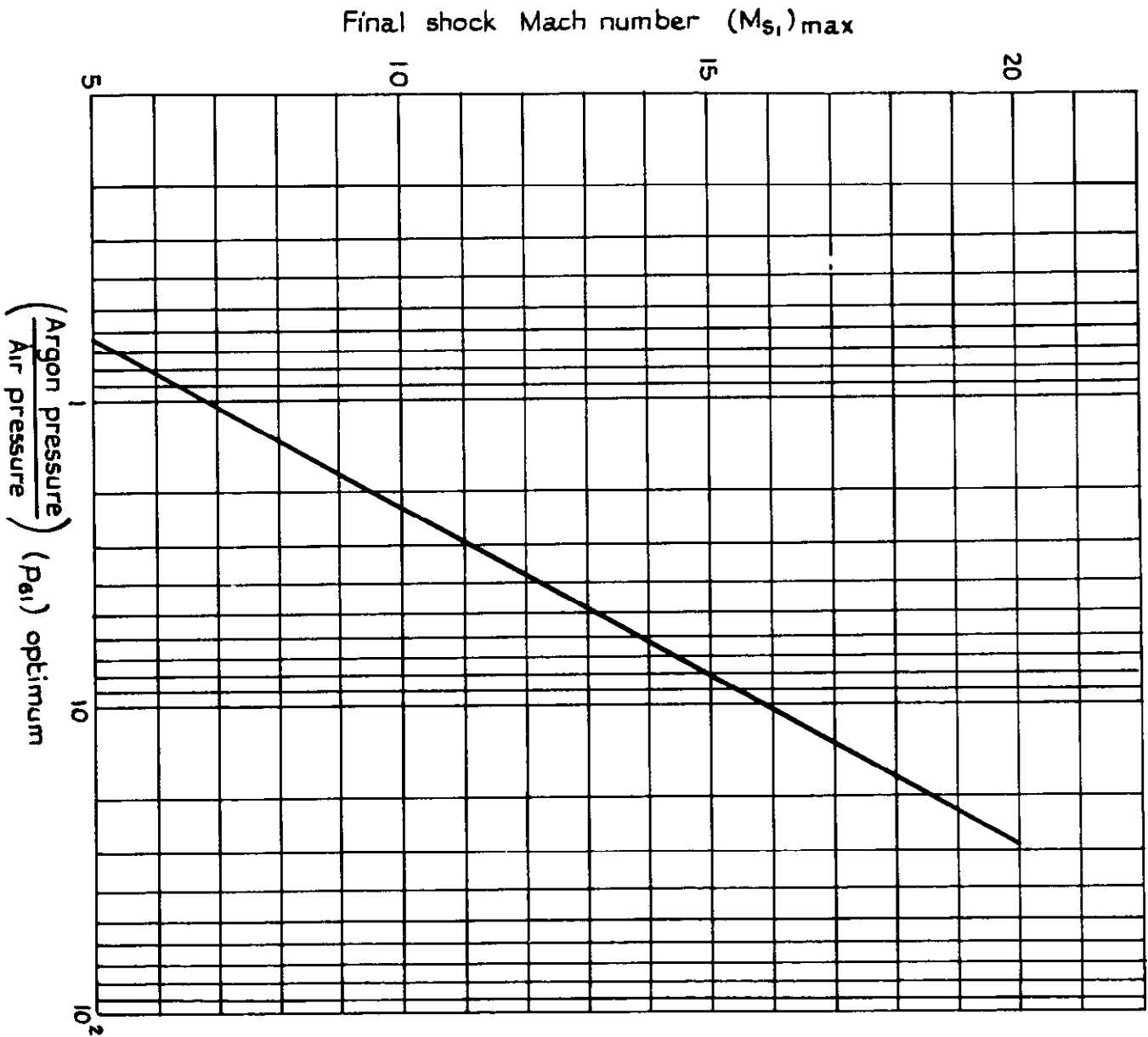
The performance of Argon → Air shock tubes.

Fig. 6.



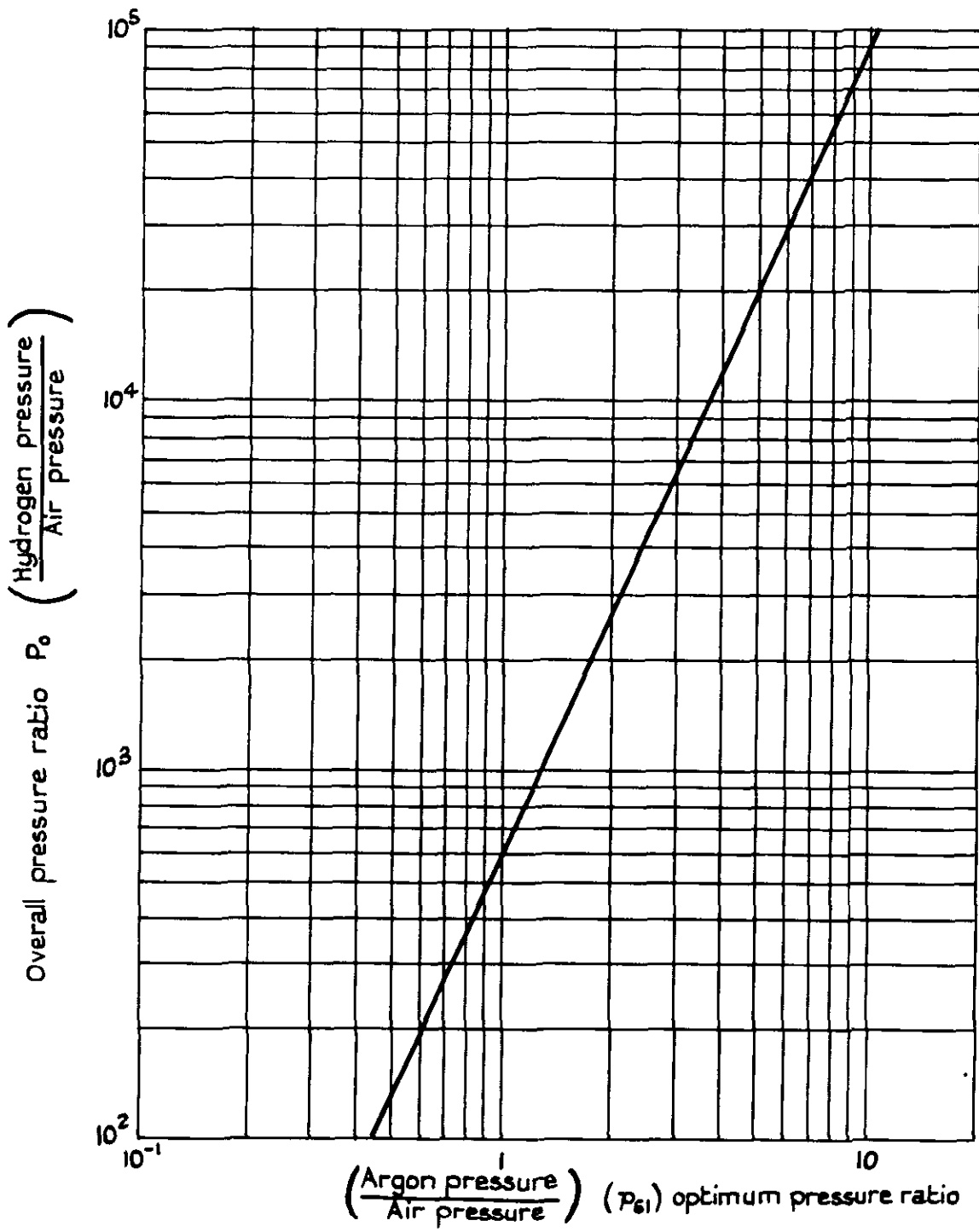
The performance of a $H_2 \rightarrow$ Argon \rightarrow Air shock tube

FIG. 7



Optimum operation of a H₂ → Argon → Air shock tube:
maximum final shock Mach number as a function of
 $\frac{\text{Argon}}{\text{Air}}$ pressure ratio.

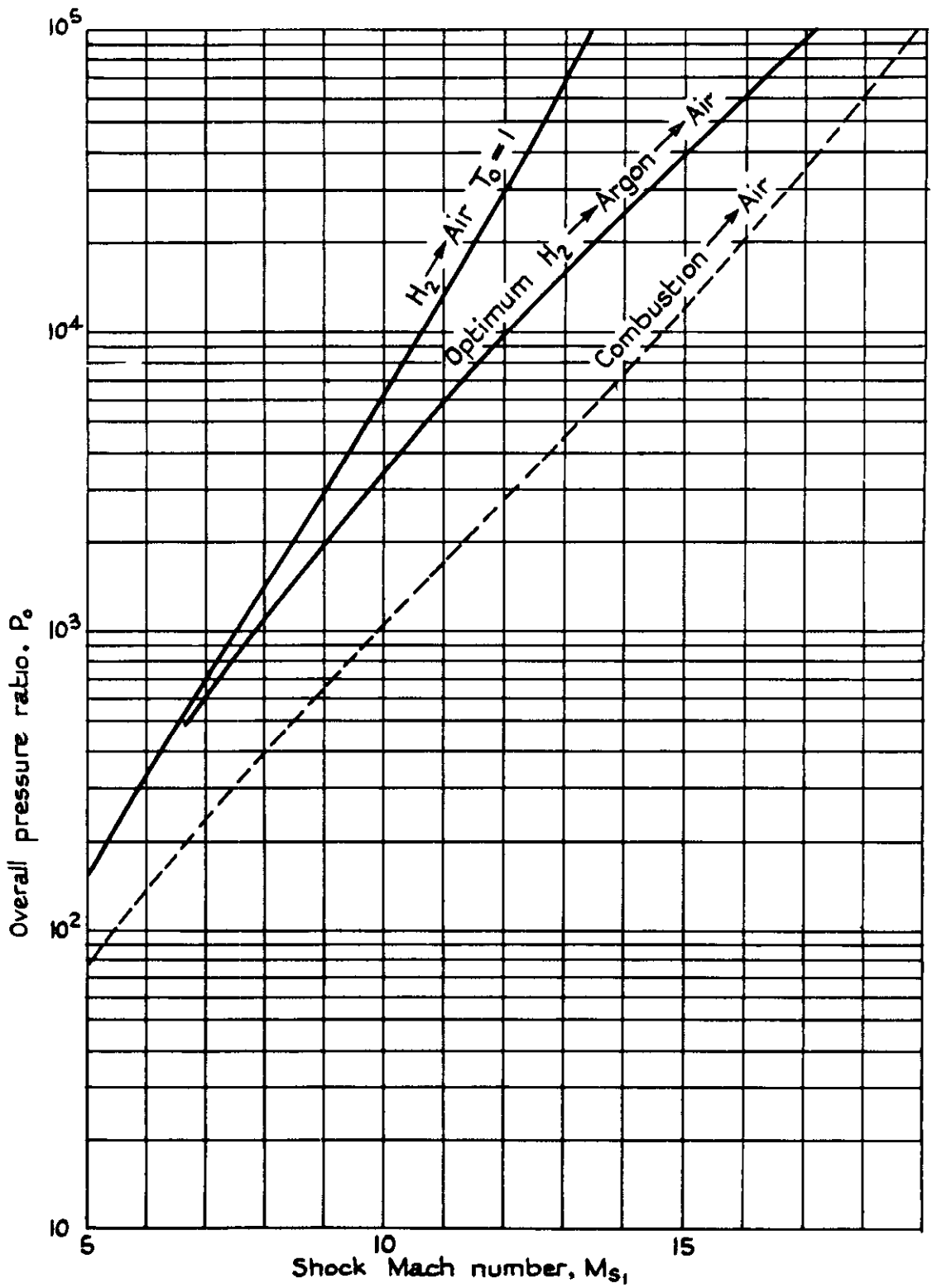
FIG 8



Optimum operation of a $H_2 \rightarrow \text{Argon} \rightarrow \text{Air}$ shock tube.

Variation of $\frac{\text{Argon}}{\text{Air}}$ pressure ratio with overall pressure ratio P_0 for maximum shock Mach number.

FIG. 9



Comparison of performances of $H_2 \rightarrow \text{Air}$; combustion $\rightarrow \text{Air}$ and the optimum $H_2 \rightarrow \text{Argon} \rightarrow \text{Air}$ shock tubes.

© *Crown copyright 1958*

Printed and published by
HER MAJESTY'S STATIONERY OFFICE

To be purchased from
York House, Kingsway, London W.C.2
423 Oxford Street, London W.1
13A Castle Street, Edinburgh 2
109 St Mary Street, Cardiff
39 King Street, Manchester 2
Tower Lane, Bristol 1
2 Edmund Street, Birmingham 3
80 Chichester Street, Belfast
or through any bookseller

Printed in Great Britain